water

MDPI

Article

Mapping of Areas Vulnerable to Flash Floods by Means of Morphometric Analysis with Weighting Criteria Applied

Marcelo Portuguez-Maurtua [1,2,3,*], Jose Luis Arumi [2,4], Alejandra Stehr [5], Octavio Lagos [2,4], Eduardo Chávarri-Velarde [3] and Daniela Rivera-Ruiz [4]

1 Doctoral Program in Water Resources and Energy for Agriculture, Universidad de Concepcion, Av. Vicente Mendez 595, Chillan 3812120, Chile
2 CRHIAM Water Research Center, Universidad de Concepción, Victoria 1295, Concepción 4070386, Chile
3 Water Resources Department, College of Agricultural Engineering, Universidad Nacional Agraria La Molina, Av. La Molina s/n, Lima 15024, Peru
4 Water Resources Department, College of Agriculture Engineering, Universidad de Concepción, Av. Vicente Mendez 595, Chillan 3812120, Chile
5 Facultad de Ingeniería, Departamentol Ingeniería Civil, Universidad de Concepción, Concepción 4070386, Chile
* Correspondence: mportuguez@lamolina.edu.pe; Tel.: +51-1-949-377-610

Abstract: Flash floods, produced by heavy seasonal rainfall and characterized by high speeds and destructive power, are among the most devastating natural phenomena and are capable of causing great destruction in very little time. In the absence of hydrological data, morphometric characterization can provide important information on preventive measures against flash floods. A priority categorization of hydrographic units in the Cañete River basin was carried out using morphometric analysis together with a weighted sum analysis (WSA) based on a statistical correlation matrix. The delineation of the drainage network was performed based on Digital Elevation Model (DEM) data from the Shuttle Radar Topography Mission (SRTM). The Cañete River basin was subdivided into 11 sub-basins, and 15 morphometric parameters were selected. The priority category (very high, high, and moderate) of each sub-basin was assigned according to the value of the composite factor obtained through WSA. The results of this analysis showed that 26.08% of the total area is under a very high flash flood risk (sub-basins 3, 9, and 11), 38.46% is under a high flash flood risk (sub-basins 5, 7, 8, and 10), and 35.45% is under a moderate flash flood risk. This study concludes that flash floods predominate in sub-basin 3 and that downstream areas present characteristics of river flooding (sub-basins 9 and 11).

Keywords: flash flood; morphometric parameter; morphometric characterization; weighted sum analysis; basin prioritization

Citation: Portuguez-Maurtua, M.; Arumi, J.L.; Stehr, A.; Lagos, O.; Chávarri-Velarde, E.; Rivera-Ruiz, D. Mapping of Areas Vulnerable to Flash Floods by Means of Morphometric Analysis with Weighting Criteria Applied. *Water* **2023**, *15*, 1053. https://doi.org/10.3390/w15061053

Academic Editor: Gwo-Fong Lin

Received: 27 January 2023
Revised: 7 March 2023
Accepted: 7 March 2023
Published: 10 March 2023

1. Introduction

Flash floods are among the most devastating natural phenomena and are capable of causing great destruction in very little time [1]. These natural disasters are most often caused by extreme rainfall events (climate change), which occur during a short time in a relatively small area, resulting in excessive discharge, landslides, and mudflows [2]. Climate change is one of the greatest threats to the entire world, affecting Earth's natural balance and ecosystems and disrupting all life [3]. This phenomenon is often measured by changes in primary variables such as temperature and precipitation [4]. The prediction and control of flash floods have been very difficult due to the highly dynamic nature of the climate and their sudden appearance; under these circumstances, a greater emphasis on prevention and protection studies in areas vulnerable to natural disasters is necessary [2].

In the absence of hydrological data, morphometric analysis can provide important information on the hydrological characteristics of a basin [5,6]. Quantitative morphometric

assessment of a basin is a very effective method for interpreting various aspects of its drainage network and evaluating its hydrological behavior [7–9]. Studies on basin sub-unit prioritization that have been conducted based on morphometric analysis have aided planners and decision-makers in the development of management plans [10–15]. Thus, to achieve good drainage basin management, it is necessary to study their morphometry [5,7].

Various studies have evaluated susceptibility to flash floods in drainage basins based on an analysis of morphometric parameters, and quantitative assessment of the morphometric characteristics of a basin has allowed its hydrological response behavior to be defined [1,9,16–20]. Remote sensing and Geographic Information Systems (GIS) are ideal tools for morphometric analysis based on the treatment and quantification of topographic data [7,9,10,21–25]. Recent publications on basin prioritization have used various methodologies such as principal component analysis (PCA) [26–29], weighted sum analysis (WSA), also known as multicriteria analysis [9,16,18,22–24,28], simple additive weighting (SAW), and the technique for order of performance by similarity to ideal solution (TOPSIS) [30]. All these methodologies, together with statistical techniques, have allowed ranked priority scores to be assigned to each sub-basin according to its relationship with flash flood risk [20]. However, there are differences among the various applied methodologies in the quantity and types of parameters used in their analyses.

This investigation aims to identify zones vulnerable to flash floods based on the characterization of morphometric parameters (linear aspects, area, and relief), use weighted sum analysis (WSA) based on a statistical correlation matrix, and set a priority category for each hydrographic unit. In addition, in the absence of hydrological data, the alternative is to use topographic data as an input to identify flash flood risk zones by analyzing morphometric characteristics. The methodology adopted in this study is to use GIS tools, programming, and statistical analysis in mapping flash flood risk zones. The results show morphometric characteristics of 11 fourth-order sub-basins with very high, high, and moderate susceptibility to flash floods. The article is organized as follows: Section 2 presents information on the location of the study area, the morphometric parameters considered, the dataset, and the methodology. Section 3 presents and discusses the results. Finally, the conclusions of this study are described in Section 4.

2. Materials and Methods

2.1. Study Area

The Cañete River basin is part of the Peruvian Pacific slope, located between geographic coordinates 11°58′ and 13°10′ south and 76°25′ and 75°30′ west, in the Cañete and Yauyos provinces, in the Department of Lima, Perú. The river basin covers an area of 6192 km^2. It has a maximum altitude of 5800 masl in the central Andes, and the river flows into the Pacific Ocean at 0 masl (Figure 1). The 79.5% of the basin located above 2500 masl is classified as wet. The Cañete River originates at Ticllacocha Lake and is located in the foothills of the Ticlla and Pichahuarco ranges at an altitude of 4429 masl. After flowing 235.67 km, with an average slope of 1.85%, it empties into the Pacific Ocean. Along its path, the Cañete River receives the contributions of numerous tributaries, including, on its right bank, the Miraflores, Yauyos, Huantuya (Carania), and Aucampi rivers and, on its left bank, the Alis, Laraos, Huantán, Tupe, Cacra, and Huangascar rivers, primarily [31,32].

2.2. Morphometric Parameters

These indicators are necessary to understand and estimate the hydrological and morphological characteristics of a basin; they also allow an interpretation of linear aspects, area, and relief of a drainage basin [1,14,15,20,33–35]. Remote sensing and Geographic Information Systems (GIS) are effective tools for delineating and understanding the morphometry of any drainage basin [7,9,35,36].

The morphometric parameters used in the study are presented in Tables 1–3.

Table 1. Linear morphometric parameters and formulas with references.

Item	Morphometric Parameter	Unit	Formula and Definition	Reference
1	Stream order (u)	Dimensionless	Hierarchical range	[37]
2	Stream length (L_u)	Km	Stream length	[38]
3	Basin length (L_b)	Km	$L_b = 1.312 \times A^{0.568}$ L_b = basin length (km) A = basin area (km^2).	[39,40]

Table 2. Morphometric parameters related to area and formulas with references.

Item	Morphometric Parameter	Unit	Formula and Definition	Reference
1	Basin area (A)	Km^2	Estimated in GIS	
2	Basin perimeter (P)	Km	Estimated in GIS	[41]
3	Stream frequency or flow frequency (F_s)	$\left(\mathrm{Km}^{-2}\right)$	$F_s = \Sigma N_u/A$ N_u = total number of stream segments of order "u" and A = basin area (km^2)	[42]
4	Drainage density (D_d)	$\left(\mathrm{Km}^{-1}\right)$	$D_d = \Sigma\, L/A$ L = total stream length; A = basin area	[42]
5	Form factor (F_f)	Dimensionless	$F_f = A/L_b^2$ A = basin area L_b = basin length	[42]
6	Circularity ratio (C_r)	Dimensionless	$C_r = 4\pi A/P^2$ A = basin area (km^2) P = basin perimeter (km)	[43]
7	Texture ratio (T_r)	Dimensionless	$Tr = N_l/P$ N_l = total number of first order streams P = basin perimeter	[38]
8	Elongation ratio (E_r)	Dimensionless	$E_r = 2\sqrt{(A/\pi)}/L_b$ A = basin area $\pi = 3.14$ L_b = basin length	[41]
9	Shape factor (S_f)	Dimensionless	$S_f = L_b^2/A$	[42]

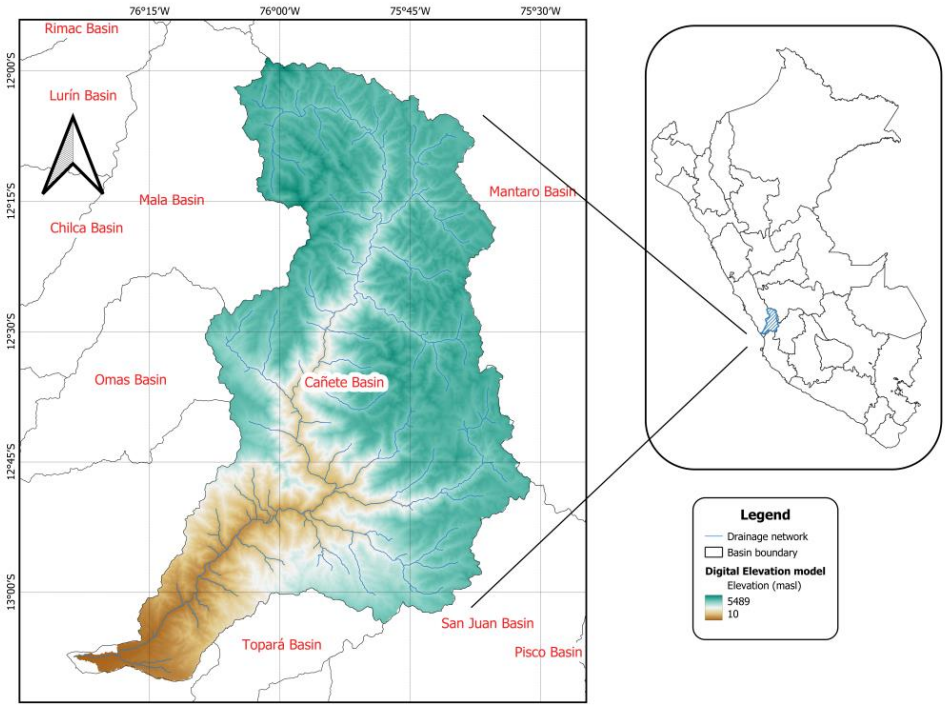

Figure 1. Map showing the location of the Cañete River drainage system.

Table 3. Morphometric parameters related to relief and formulas with references.

Item	Morphometric Parameter	Unit	Formula and Definition	Reference
1	Basin relief *(R)*	Meters	$R = H - h$ R = basin relief, H = maximum elevation in meters H = minimum elevation in meters	[41]
2	Relief ratio (R_r)	Dimensionless	$R_r = H/L_b$ R_r = relief ratio, H = basin relief, L_b = basin length	[41]
3	Average slope (A_s)	Degrees	Estimated in GIS	

2.3. Data Used

In this study, Shuttle Radar Topography Mission (SRTM) Digital Elevation Model (DEM) data were used to delineate the basin, extract the drainage/stream network, and subdivide the catchment area into sub-basins. The SRTM V3 (SRTM Plus) product is provided by the National Aeronautics and Space Administration (NASA) and has a resolution of 1 arc-second (approximately 30 m) [44].

The DEMs were downloaded from Google Earth Engine (GEE), a cloud-based platform that facilitates access to a catalog of petabytes of publicly available geospatial data, including satellite and aerial images, environmental, meteorological, climate, and topographic variables, land cover, etc. [45–47]. GEE is accessed using an application programming interface (API) accessible by the internet and an associated web-based integrated development environment (IDE) that allows the quick creation of prototypes and visualization of results [45,47–49]. In this study GEE was accessed using the Kaggle web platform, which offers a customizable Jupyter Notebooks interface, using Python programming language [50]. A rectangular region that covers the entire Cañete River basin was downloaded. Data Availability shows the codes that were used.

2.4. Methodology

The methodology adopted in this study is described by the following steps: (1) Extraction of drainage network and sub-basin delineation. (2) Morphometric analysis using the QGIS tool. (3) Assignment of preliminary ranking of sub-basin priority. (4) Weighted sum analysis and final ranking, y. (5) Mapping of areas vulnerable to flash floods. Figure 2 presents the methodological diagram of this research.

2.4.1. Extraction of Drainage Network and Sub-Basin Delineation

The drainage network extraction and basin delineation were carried out following DEM processing methods (cell filling, flow direction, flow accumulation, *stream order* definition, stream segmentation, and basin delineation) using the QSWAT complement in QGIS 3.16 [51,52]. To define the streams in the study area, a threshold value corresponding to 1% (192,777 cells) of the DEM cell count was used. The Cañete River basin was subdivided into 11 sub-basins, designated as SC-1 to SC-11, and the entire drainage network was classified as a fourth-order catchment basin using the Strahler method [37].

2.4.2. Morphometric Analysis

A morphometric analysis is necessary to ascertain the sub-basin prioritization. This process is advantageous as the derived basin variables are in the form of ratios or dimensionless numbers, providing an effective comparison independent of scale [1,14,14,20,24,34,35]. Morphometric analysis offers a complete representation of the drainage network, geometry, and topography of the basin, allowing an interpretation of linear aspects, area, and relief of the basin, respectively [9].

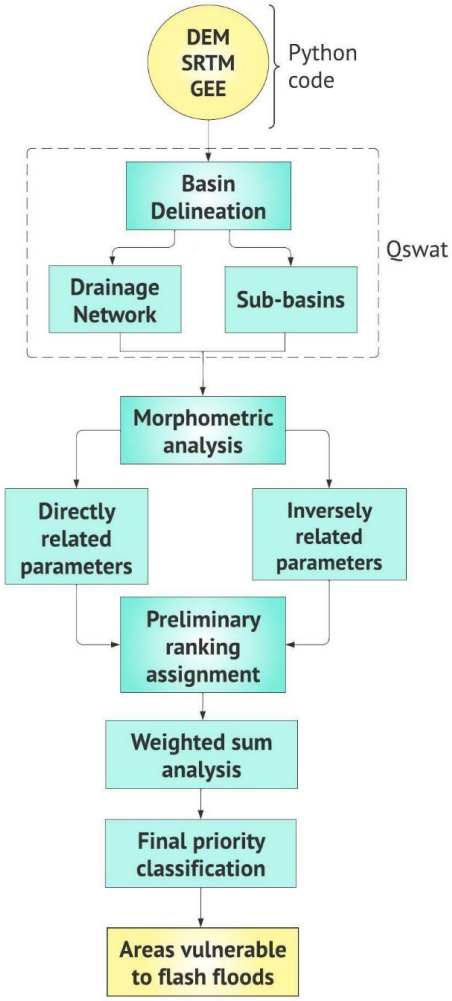

Figure 2. Methodological diagram for mapping of areas vulnerable to flash floods.

Each of these parameters can directly or indirectly influence the surface runoff of the drainage basin [9], facilitating the understanding of how they influence flash flood risk. Tables 1–3 show a list of morphometric parameters that describe the dimensionless and multidimensional characteristics of the basin, which are grouped into 3 aspects. First, linear morphometric characterization: *stream order (u)*, *stream length* (L_u), and *basin length* (L_b), shown in Table 1 [37–39]. Second, morphometric characterization of area: *basin area (A)*, *basin perimeter* (*P*), stream frequency, also known as *flow frequency* (F_s), *drainage density* (D_d), *form factor* (F_f), *circularity ratio* (C_r), drainage texture (T_r), *elongation ratio* (E_r), and *shape factor* (S_f), shown in Table 2 [38,41–43]. Finally, *basin relief (R)*, *relief ratio* (R_r), and *average slope* (A_s) are morphometric relief parameters, shown in Table 3 [41].

2.4.3. Preliminary Ranking of Sub-Basin Priority

The preliminary ranking (PR) approach was used, in which morphometric parameters were divided into two groups according to their ability to (directly or indirectly) influence the adversity of the morphometric parameter conditions or degree of susceptibility to flash floods [16,18,19,22,24]. The first group of parameters (capable of direct influence) consisted of: *basin relief (R)*, *relief ratio* (R_r), *drainage density* (D_d), stream frequency (F_s), *circularity ratio* (C_r), drainage texture (T_r), and *average slope* (A_s). The second group of parameters (capable of indirect influence) consisted of: *elongation ratio* (E_r), *form factor* (F_f), and *shape factor* (S_f).

The preliminary rankings of the parameters in the first group were assigned in such a way that for each parameter the sub-basin with the highest value was classified as 1, that with the next highest value was classified as 2, and so on for the remaining sub-basins. The

opposite was done for the parameters in the second group, assigning rankings in such a way that for each parameter the sub-basin with the lowest value was placed in position 1, that with the next lowest value was placed in position 2, and so on for the remaining sub-basins [16,18,22].

2.4.4. Weighted Sum Analysis and Final Ranking

Weighted sum analysis (WSA) is a well-known method that provides consistency in addressing complicated problems to compare land surface processes in related entities such as drainage basins [26]. WAS, also known as multi-criteria decision making, is widely used to select the best alternatives among multiple options. Based on preliminary rankings, the correlation matrix and correlation coefficients were calculated [16,18]. The composite parameters (WSA_{cp}) were calculated using the following equation (Equation (1)) [9,16,22,26]:

$$WSA_{cp} = PR_{p1} \times W_{p1} + PR_{p2} \times W_{p2} + \ldots + PR_{pn} \times W_{pn} \quad (1)$$

where WSA_{cp} = composite parameter used for weighted sum analysis; PR = preliminary priority ranking of each morphometric parameter ($p1$, $p2$, … pn); and W = weights of the morphometric parameters obtained by means of the correlation matrix, which was calculated using the following equation (Equation (2)):

$$Parameter\ weights\ (W) = \frac{Correlation\ coefficient\ sum}{Correlation\ total} \quad (2)$$

Therefore, sub-basin priority was assigned by taking the $WSA_{cp}(+)$ values (capable of direct influence) corresponding to the first group and subtracting the $WSA_{cp}\ (-)$ values (capable of direct influence) corresponding to the second group, following the equation (Priority $= WSA_{cp}(+) - WSA_{cp}(-)$). Subsequently, final ranking values were assigned, one for the lowest priority value, two for the following value, and so on. Finally, to categorize the priority type, the maximum category (very high) corresponds to the lowest priority levels [9,18,22]. Finally, a model was formulated to assess the final priority using the WSA_{cp} value of each parameter, as shown below:

$$Priorizacion = (R + R_r + D_d + F_s + C_r + T_r + A_s) - \left(E_r + F_f + S_f\right) \quad (3)$$

3. Results and Discussion

The identification of areas in drainage basins vulnerable to flash floods using morphometric parameters is considered one of the most effective methods to characterize various geohydrological properties of a basin [14,24]. Therefore, this study has used different morphometric parameters that govern the hydrological response of a basin to prioritize the sub-basins of the Cañete River in terms of their vulnerability to flash floods.

3.1. Morphometric Analysis of the Basin

The morphometric analysis was carried out for 11 sub-basins, and the drainage network of the entire study area was considered a fourth-order basin (Figure 3). The morphometric analysis covered 15 parameters for each sub-basin, which was necessary to determine its dimensions, shape and area, and the characteristics of the drainage network. The results reveal that SB-9 is the smallest, with an area of 31.49 km^2, while SB-11 is the largest, with an area of 1175.47 km^2 (Table 4). More than half of the sub-basins have areas greater than 400 km^2, with only SB-9 having an area smaller than 50 km^2. Most of the sub-basins are large, with areas greater than 300 km^2. The area of a sub-basin directly affects its susceptibility to flash floods [16,19].

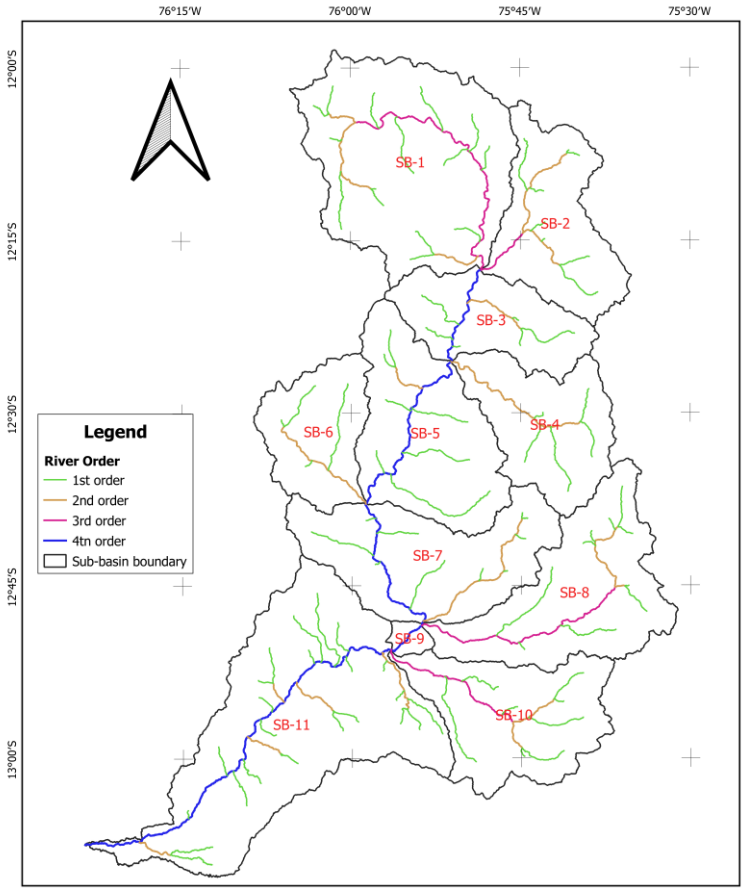

Figure 3. Sub-basins and drainage network of the Cañete River.

Table 4. Area, perimeter, and length of each sub-basin.

Sub-Basin	Perimeter (km)	Area (km^2)	Length (km)
SB-1	197.09	943.30	64.20
SB-2	158.45	448.58	42.09
SB-3	137.14	364.68	37.42
SB-4	145.79	419.96	40.54
SB-5	162.71	586.76	49.03
SB-6	118.83	324.56	35.02
SB-7	183.65	596.71	49.50
SB-8	204.97	616.61	50.43
SB-9	30.01	31.49	9.31
SB-10	167.51	517.64	45.66
SB-11	281.88	1175.47	72.75

Basin perimeter (P) values for the study area vary from 30.01 km (SB-9) to 281.88 km (SB-11). *Basin length* (L_b) is understood as the maximum length and is calculated from the farthest point on the basin border to the confluence point; the values vary from 9.31 km (SB-9) to 72.75 km (SB-11). The values are presented in Table 4.

Figure 3 and Table 5 show that there are 97 first-order streams, 41 second-order streams, 18 third-order streams, and 37 fourth-order streams. Table 5 also shows that the greatest number of streams was found in SB-11 (49), and the smallest number of streams was found in SB-9 (1).

Table 5. Number of streams in each sub-basin by stream order.

Stream Order (u)	SB-1	SB-2	SB-3	SB-4	SB-5	SB-6	SB-7	SB-8	SB-9	SB-10	SB-11
1st order	15	8	6	5	7	4	10	10	0	8	24
2nd order	5	6	2	4	1	3	4	5	0	3	8
3rd order	9	1	0	0	0	0	0	4	0	4	0
4th order	0	0	5	0	7	0	7	0	1	0	17
Total	29	15	13	9	15	7	21	19	1	15	49

Table 6 shows the lengths of the first- to fourth-order streams of the 11 sub-basins, determined using the GIS technique [51], which indicates that the total length of all streams varies from a minimum of 7.68 km (SB-9) to a maximum of 247.19 km (SB-11), and that the total length of all streams in the basin is 1113.75 km. The drainage length values show a significant interrelationship with drainage flow discharge and the erosion phase of the river basin [18]. In addition, it is seen that the five sub-basins with fourth-order streams (SB-3, SB-5, SB-7, SB-9, and SB-11) are possibly susceptible to flash floods [16,19]. Drainage length is a parameter that is directly related to the hydrological reaction of a watershed and its importance is approximately equal to half the reciprocal of the *drainage density* [19].

Table 6. Stream length in each sub-basin by stream order.

Stream Order (u)	SB-1 (km)	SB-2 (km)	SB-3 (km)	SB-4 (km)	SB-5 (km)	SB-6 (km)	SB-7 (km)	SB-8 (km)	SB-9 (km)	SB-10 (km)	SB-11 (km)
1st order	88.01	35.04	32.84	36.10	66.93	29.11	41.07	54.75	0.00	59.13	128.42
2nd order	31.80	29.39	11.92	30.52	7.66	22.31	29.79	17.16	0.00	14.11	39.91
3rd order	54.55	10.43	0.00	0.00	0.00	0.00	0.00	41.79	0.00	28.51	0.00
4th order	0.00	0.00	19.35	0.00	36.67	0.00	29.95	0.00	7.68	0.00	78.86
Total	174.36	74.86	64.11	66.62	111.26	51.43	100.80	113.70	7.68	101.74	247.19

Drainage density (D_d) and stream frequency (F_s) were calculated for all sub-basins (Table 7). In the analysis of the sub-basin and drainage network map (Figure 3), the Cañete River basin was found to be a fourth-order basin, with a dendritic drainage pattern. D_d and F_s are significant parameters that contribute to the hydrological responses in each sub-basin [19]. The F_s and D_d values in each sub-basin are directly proportional; therefore, a greater stream number corresponds to a greater stream length. The high value of F_s in sub-basins 3, 7, and 11 indicates that they produce more runoff in comparison to the other sub-basins. Meanwhile, high D_d values are observed in sub-basins 9 and 11, indicating a well-developed network, which is conducive to high runoff concentrations that give rise to flash floods. The low value of D_d in sub-basins 4 and 6 indicates that they have highly permeable subsoil material, with dense plant cover and a low relief [53]. Therefore, high values of D_d and F_s are likely to increase susceptibility to high surface runoff and flash floods [19].

Table 7. Morphometric parameters that represent area and form aspects of the sub-basins.

Sub-Basin	Drainage Density (D_d)	Stream Frequency (F_s)	Circularity Ratio (C_r)	Texture Ratio (T_r)	Elongation Ratio (E_r)	Form Factor (F_f)	Shape Factor (S_f)
SB-1	0.185	0.031	0.305	0.076	0.540	0.229	4.369
SB-2	0.167	0.033	0.225	0.050	0.568	0.253	3.949
SB-3	0.176	0.036	0.244	0.044	0.576	0.260	3.840
SB-4	0.159	0.021	0.248	0.034	0.570	0.255	3.914
SB-5	0.190	0.026	0.279	0.043	0.558	0.244	4.096
SB-6	0.158	0.022	0.289	0.034	0.580	0.265	3.779
SB-7	0.169	0.035	0.222	0.054	0.557	0.244	4.106
SB-8	0.184	0.031	0.184	0.049	0.556	0.242	4.124
SB-9	0.244	0.032	0.439	0.000	0.680	0.363	2.752
SB-10	0.197	0.029	0.232	0.048	0.562	0.248	4.027
SB-11	0.210	0.042	0.186	0.085	0.532	0.222	4.502

The *circularity ratio* (C_r) is influenced by *stream length* and frequency, geological structures, land use and cover, climate, relief, and basin slope [35]. For a perfectly circular basin, the value of the *circularity ratio* is 1 [43]. In this study, the C_r values of the sub-basins range from 0.184 to 0.439 (Table 7); all the values are less than 1, which indicates that the area is characterized by an elevated relief and that the drainage system is structurally controlled.

Infiltration capacity is the only important factor that controls the *texture ratio* (T_r) [9]. The texture ratio in the sub-basins range from 0.00 to 0.085 (Table 7). The highest relief values are attributed to the pronounced slopes of the sub-basins, which makes them more prone to flood risk [16,24]. Meanwhile, the lowest Tr values indicate that the basin is flat, with slope values close to zero degrees [35].

The *elongation ratio* (E_r) is the measure of basin dimensions or basin shape [41]. According to [37], a sub-basin with an Er value above 0.9 is classified as circular, those with Er values between 0.9 and 0.8 are classified as oval, those with Er values between 0.7 and 0.8 are classified as less elongated, those with Er values between 0.5 and 0.7 are classified as elongated, and those with Er values below 0.5 are classified as more elongated. In this study, the Er values vary between 0.532 and 0.680, indicating that the sub-basins are classified as elongated.

The *form factor* (F_f) is a dimensionless ratio of the area of a basin to the square of its length [42] and can be effectively related to flood occurrence, erosion intensity, and sediment transport capacity in a basin [1]. The lower the *form factor* value, the longer the basin. Basins with a high *form factor* have high, short-duration maximum flows, while those with a low *form factor* have lower, longer-duration maximum flows [16,35]. In this study the sub-basins have Ff values ranging from 0.222 to 0.363 (Table 7), indicating that they have elongated shapes and suggesting lower, longer-duration maximum flows.

The *shape factor* (S_f) is a dimensionless ratio of the square of the length of a basin to its area [42]. Its values indicate the opposite of those of Ff, with a maximum Sf value corresponding to a minimum Ff value. The Sf values for each sub-basin vary between 2.752 (SB-9) and 4.502 (SB-11) (Table 7).

Basin relief (*R*) is defined as the change between its highest- and lowest-elevation points [9,18]. Table S1 (Supplementary Materials) details the minimum and maximum height values and other statistics for each sub-basin. R shows the potential energy of a drainage basin, which significantly influences the channel gradient and aspect and landform evolution; therefore, it directly affects surface runoff, flood patterns, and sediment transport [9,18,24]. The highest and lowest R values are found in SB-11 (4420.00 m) and SB-2 (2061.00 m) (Table 8). Maximum R values are indicative of the potential energy of a given sub-basin to move water and sediment along the slope.

Table 8. Morphometric parameters that represent sub-basin relief aspects.

Sub-Basin	Basin Relief (*R*) (m)	Relief Ratio (R_r)	Average Slope (A_s) (°)
SB-1	2906.00	0.045	22.590
SB-2	2061.00	0.049	20.816
SB-3	3287.00	0.088	27.833
SB-4	2844.00	0.070	22.800
SB-5	4127.00	0.084	27.959
SB-6	3309.00	0.094	19.485
SB-7	4063.00	0.082	27.023
SB-8	4156.00	0.082	22.011
SB-9	2405.00	0.258	34.042
SB-10	3963.00	0.087	21.225
SB-11	4420.00	0.061	23.243

The *relief ratio* (R_r) is estimated as the ratio of *basin relief* to *basin length*. According to [41], there is a correlation between the hydrological characteristics of a basin and the *relief ratio*. Therefore, it is presented as an indicator of the intensity of the erosion process in

the basin [9,16]. High R values are characteristic of mountainous regions. The R values for all the sub-basins (Table 8) are between 0.045 (SB-1) and 0.258 (SB-9). *Average slope* refers to the amount of inclination of the physical feature or the topographic form with respect to the horizontal. Table S2 (Supplementary Materials) details the slope raster statistics in degrees for each sub-basin. Slope analysis is very important in morphometric studies. Slope elements are, in turn, controlled by climate-morphogenic processes in areas with rocks of varying resistance [1,54]. The average slopes of the sub-basins vary from 19.485° (SB-6) to 34.042° (SB-9) (Table 8). The pronounced slopes also favor a faster movement of surface runoff.

3.2. Assignment of Preliminary Sub-Basin Priority Rankings

The seven morphometric parameters (R, R_r, D_d, F_s, C_r, T_r, and A_s) are directly proportional to soil degradation and water factors. The rankings were assigned from greatest to lowest priority, i.e., rank 1 for the sub-basin with the maximum parameter value and rank 11 for the sub-basin with the minimum parameter value. For example, parameter R (Table 8) with the maximum value of 4420.0 m (SB-11) was assigned the highest priority (rank 1), the next descending value was assigned rank 2, and this went up to the minimum parameter value of 2061.0 m (SB-2), which was assigned the lowest priority (rank 11). The assignment of the rankings for the six parameters R_r, D_d, F_s, C_r, T_r, and A_s was assigned in a similar way as explained above, the results are shown in Table 9.

Table 9. Preliminary priority rankings.

Sub-Basin	R	R_r	D_d	F_s	C_r	T_r	A_s	E_r	F_f	S_f
SB-1	8	11	5	7	2	2	7	2	2	10
SB-2	11	10	9	4	8	4	10	7	7	5
SB-3	7	3	7	2	6	7	3	9	9	3
SB-4	9	8	10	11	5	9	6	8	8	4
SB-5	3	5	4	9	4	8	2	5	5	7
SB-6	6	2	11	10	3	10	11	10	10	2
SB-7	4	7	8	3	9	3	4	4	4	8
SB-8	2	6	6	6	11	5	8	3	3	9
SB-9	10	1	1	5	1	11	1	11	11	1
SB-10	5	4	3	8	7	6	9	6	6	6
SB-11	1	9	2	1	10	1	5	1	1	11

The three remaining parameters (E_r, F_f, and S_f) have an inverse relationship with soil degradation and water factors. Rankings were assigned from lowest to highest priority, i.e., rank 1 for the sub-basin with the lowest parameter value and rank 11 for the sub-basin with the highest parameter value. For example, parameter E_r (Table 7) with a minimum value of 0.532 (SB-11) was assigned the highest priority (rank one), and the next higher value was assigned rank two; the maximum parameter value of 0.680 (SB-9) was assigned the lowest priority (rank 11). The assignment of the rankings for the next two parameters (F_f and S_f) were similarly assigned, the results are shown in Table 9.

A correlation matrix of the 10 morphometric parameters capable of directly or indirectly influencing the vulnerability to flash floods is presented in Table 10. It was estimated based on the preliminary priority rankings (Table 9), and the correlation coefficients were obtained in a process carried out using Python code (Data Availability shows the codes used). The statistical correlation matrix shows that *basin relief* has a positive correlation with *relief ratio*, *drainage density*, stream frequency, *texture ratio*, *average slope*, *elongation ratio*, and *form factor* and an inverse correlation with *circularity ratio* and *shape factor*. The *relief ratio* has a positive correlation with *basin relief*, *drainage density*, *circularity ratio*, *average slope*, and *shape factor* and an inverse correlation with stream frequency, *texture ratio*, *elongation ratio*, and *form factor*. The *drainage density*, stream frequency, *circularity ratio*, *texture ratio*, *average slope*, *elongation ratio*, *form factor*, and *shape factor* correlations were also calculated and are shown in Table 10.

Table 10. Correlation matrix of the morphometric parameters.

	R	R_r	D_d	F_s	C_r	T_r	A_s	E_r	F_f	S_f
R	1.000	0.009	0.282	0.173	−0.564	0.373	0.082	0.636	0.636	−0.636
R_r	0.009	1.000	0.136	−0.155	0.345	−0.782	0.255	−0.709	−0.709	0.709
D_d	0.282	0.136	1.000	0.327	0.064	0.145	0.518	0.282	0.282	−0.282
F_s	0.173	−0.155	0.327	1.000	−0.482	0.564	0.318	0.282	0.282	−0.282
C_r	−0.564	0.345	0.064	−0.482	1.000	−0.600	0.227	−0.545	−0.545	0.545
T_r	0.373	−0.782	0.145	0.564	−0.600	1.000	−0.173	0.873	0.873	−0.873
A_s	0.082	0.255	0.518	0.318	0.227	−0.173	1.000	−0.064	−0.064	0.064
E_r	0.636	−0.709	0.282	0.282	−0.545	0.873	−0.064	1.000	1.000	−1.000
F_f	0.636	−0.709	0.282	0.282	−0.545	0.873	−0.064	1.000	1.000	−1.000
S_f	−0.636	0.709	−0.282	−0.282	0.545	−0.873	0.064	−1.000	−1.000	1.000
Sum	1.991	0.100	2.755	2.027	−0.555	1.400	2.164	1.755	1.755	−1.755
Weight (w)	0.171	0.009	0.237	0.174	−0.048	0.120	0.186	0.151	0.151	−0.151

The final weights for each parameter were calculated by dividing the correlation coefficient sum of each parameter by the overall correlation total (Equation (2)). The final weight of R (weight = 0.171) was obtained though division (1.991/11.636). The final weights of the other morphometric parameters were obtained in a similar manner; the results are shown at the bottom of Table 10. The value 11.636 was obtained by summing the sum row (penultimate row Table 10).

3.3. Final Ranking Using Weighted Sum Analysis

The WSA_{cp} values of the morphometric parameters (Equation (1)) were calculated according to their importance using the weighted sum model. This process used the preliminary priority values (Table 9) and final weights of each morphometric parameter (Table 10). For example, the WSA_{cp} value of R (SB-1) was obtained by multiplying 8 × 0.171 = 1.37, and similarly for the following WSA_{cp} values of R of the other sub-basins; WSA_{cp} of R_r was multiplied 11 × 0.009 = 0.09. Therefore, for each parameter there is a corresponding weighting (w). The WSA_{cp} values are shown in Table 11.

Table 11. WSA_{cp} values in each sub-basin.

Sub-Basin	R	R_r	D_d	F_s	C_r	T_r	A_s	E_r	F_f	S_f
SB-1	1.37	0.09	1.18	1.22	−0.10	0.24	1.30	0.30	0.30	−1.51
SB-2	1.88	0.09	2.13	0.70	−0.38	0.48	1.86	1.06	1.06	−0.75
SB-3	1.20	0.03	1.66	0.35	−0.29	0.84	0.56	1.36	1.36	−0.45
SB-4	1.54	0.07	2.37	1.92	−0.24	1.08	1.12	1.21	1.21	−0.60
SB-5	0.51	0.04	0.95	1.57	−0.19	0.96	0.37	0.75	0.75	−1.06
SB-6	1.03	0.02	2.60	1.74	−0.14	1.20	2.05	1.51	1.51	−0.30
SB-7	0.68	0.06	1.89	0.52	−0.43	0.36	0.74	0.60	0.60	−1.21
SB-8	0.34	0.05	1.42	1.05	−0.52	0.60	1.49	0.45	0.45	−1.36
SB-9	1.71	0.01	0.24	0.87	−0.05	1.32	0.19	1.66	1.66	−0.15
SB-10	0.86	0.03	0.71	1.39	−0.33	0.72	1.67	0.90	0.90	−0.90
SB-11	0.17	0.08	0.47	0.17	−0.48	0.12	0.93	0.15	0.15	−1.66

Based on the results of the composite weighted sum WSA_{cp} of the different parameters (Table 11), a model was formulated to evaluate the final priority ranking (equation 3). The parameters were categorized into two groups: first group WSA_{cp} $(+)$, parameters that have the ability to directly influence flash floods; second group, WSA_{cp} $(-)$, parameters that have the ability to indirectly influence flash floods. The priorities ranking (prioritization) is obtained by subtracting the two groups WSA_{cp} $(+)$ − WSA_{cp} $(-)$; the sub-basin with the lowest composite value receives the highest priority (one), that with the next lowest composite value receives the second rank, and so on for the classification of each hydrological unit.

The final classification of priorities was carried out in such a way that the lowest composite factor value received priority rank 1, the next lowest value received priority rank 2, and so on for the 11 sub-basins. As observed in Table 12, the highest priority rank (1) was assigned to SB-9, followed by SB-3, SB-11, SB-5, SB-7, SB-10, SB-8, SB-2, SB-6, SB-4, and SB-1. Figure 4 shows the final map of priority classifications of the 11 studied sub-basins.

Table 12. Final ranking and sub-basin priority areas.

Sub-Basin	WSA_{cp} (+)	WSA_{cp} (−)	Priority	Priority Level	Priority Type	Area (%)
SB-1	5.31	−0.90	6.22	11	Medium	15.65
SB-2	6.75	1.36	5.40	8	Medium	7.44
SB-3	4.34	2.26	2.08	2	Very high	6.05
SB-4	7.85	1.81	6.04	10	Medium	6.97
SB-5	4.21	0.45	3.76	4	High	9.74
SB-6	8.50	2.71	5.78	9	Medium	5.39
SB-7	3.84	0.00	3.84	5	High	9.90
SB-8	4.42	−0.45	4.88	7	High	10.23
SB-9	4.29	3.17	1.12	1	Very high	0.52
SB-10	5.06	0.90	4.15	6	High	8.59
SB-11	1.47	−1.36	2.83	3	Very high	19.51

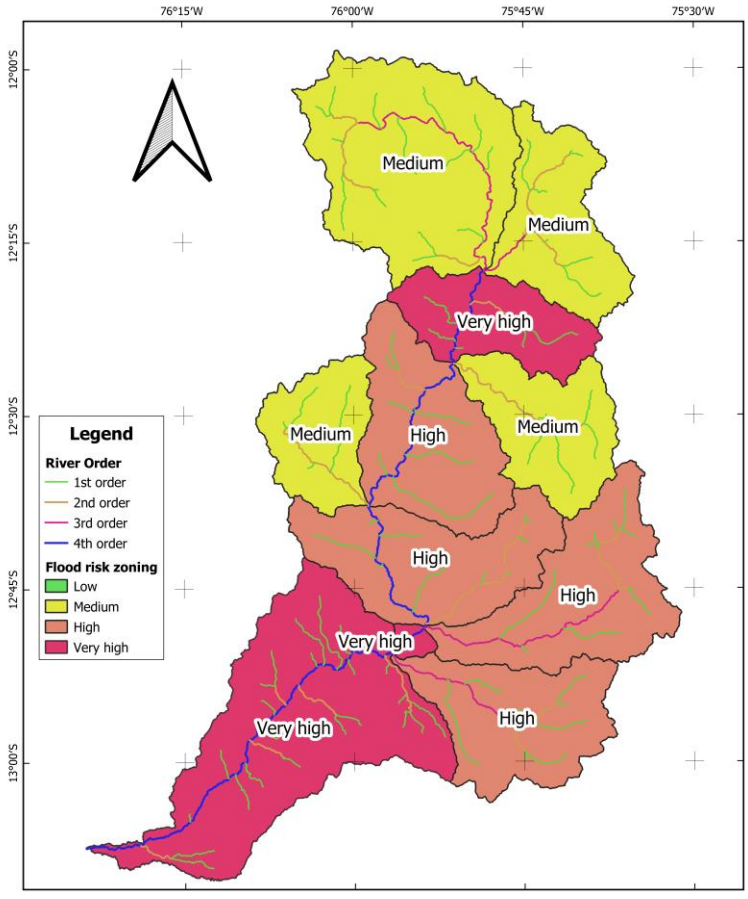

Figure 4. Map of zones vulnerable to flash floods in the Cañete basin.

From the results shown in Table 12, there are composite parameter values WSA_{cp} that have the ability to directly or indirectly influence the degree of susceptibility to flash floods. Based on the composite factor value, the 11 sub-basins of the Cañete River basin were classified into three priority categories: very high, high, and medium [9]. In Table 12 it can be seen that three sub-basins (SB-9, SB-3, and SB-11) are in the "very high" category, four sub-basins (SB-5, SB-7, SB-10, and SB-8) are in the "high" category, and four sub-basins (SB-2, SB-6, SB-4, and SB-1) are in the "medium" category. The final priority category map of the 11 sub-basins (Figure 4) shows that the "very high" category accounts for 26.08% of the total area, the "high" category for 38.46%, and the "medium" category for 35.45%.

These results show that 64.55% of the sub-basins (seven sub-basins) are in zones with a very high or high propensity to soil erosion, indicating that there are potential areas to carry out soil protection measures for efficient basin management and development. In addition, with the final priority classification of the 11 sub-basins (Figure 4), and considering the

continuity of the flow wave or flood that starts in SB-3 and moves downstream and is produced by a maximum rainfall event over the central region of the sub-basin, SB-5 and SB-7 could also be considered very high categories, as they follow the continuity of SB-3. Therefore, these results will be of great help to policy-makers, planners, and managers to address vulnerable areas through specific action plans for flood risk reduction.

4. Conclusions

Through the morphometric characterization carried out by interpreting the linear, area, and relief aspects of a hydrological basin, it was possible to identify areas vulnerable to flash floods in the occurrence of extreme events, as a methodological technique in basins with an absence of hydrological data and to know the hydrological behavior in a basin. In addition, the important role of GIS tools and statistical approaches in developing research was shown.

The results show that SB-3, SB-9, and SB-11 are susceptible to floods and soil loss. Flash floods predominate in the upstream sub-basin (SB-3), while the downstream sub-basin (SB-9 and SB-11) present characteristics of river floods. Both are destructive in the study area, affecting the human population and their residential units, farmland with standing crops, and infrastructure (highways, bridges, sewers, and water supply systems).

In addition, the sub-basins located in the middle part of the basin (SB-5, SB-7, SB-8, and SB-10) are categorized as high risk and the remaining sub-basins (SB-1, SB-2, SB-4, and SB-6) as medium risk. Thus, the Cañete River basin has sub-basins that present a very high, high, and moderate susceptibility to flash floods. Finally, it can be affirmed that the hydrological response and specifically the risk of flash floods and extreme events in a river basin depends on its morphometric characteristics. Therefore, this methodology is presented as an alternative to decision-makers in the application of suitable drainage basin management techniques in terms of soil and water conservation measures, allowing them to safeguard the study area and mitigate its degradation.

Supplementary Materials: The following supporting information can be downloaded at: https://www.mdpi.com/article/10.3390/w15061053/s1; Table S1: DEM statistics for each sub-basin; Table S2: raster statistics of slope in grade for each sub-basin. Python codes: CorrelationAnalysis and DownloadDEM_CodeKaggle.

Author Contributions: Conceptualization, M.P.-M. and J.L.A.; methodology, M.P.-M.; software, M.P.-M.; validation, M.P.-M. and J.L.A.; formal analysis, M.P.-M. and D.R.-R.; investigation, M.P.-M., J.L.A., A.S., O.L., E.C.-V. and D.R.-R.; writing—original draft preparation, M.P.-M. and D.R.-R.; writing—review and editing, M.P.-M., J.L.A., A.S., O.L., E.C.-V. and D.R.-R.; visualization, M.P.-M., E.C.-V. and D.R.-R.; supervision, J.L.A. and A.S. All authors have read and agreed to the published version of the manuscript.

Funding: This research was supported by the CRHIAM Water Research Center: ANID/FONDAP/15130015.

Data Availability Statement: The data presented in this study are openly available at Supplementary Materials codes, time series, algorithms, and others.

Acknowledgments: CRHIAM Water Research Center: Project ANID/FONDAP/15130015, Josselyn Portuguez Contreras, and Mariam De la Cruz.

Conflicts of Interest: The authors declare no conflict of interest. The funders had no role in the design of the study; in the collection, analyses, or interpretation of data; in the writing of the manuscript; or in the decision to publish the results.

References

1. Bisht, S.; Chaudhry, S.; Sharma, S.; Soni, S. Assessment of flash flood vulnerability zonation through Geospatial technique in high altitude Himalayan watershed, Himachal Pradesh India. *Remote Sens. Appl. Soc. Environ.* **2018**, *12*, 35–47. [CrossRef]
2. Cahyono, C.; Adidarma, W.K. Influence analysis of peak rate factor in the flood events' calibration process using HEC-HMS. *Model. Earth Syst. Environ.* **2019**, *5*, 1705–1722. [CrossRef]

3. Teng, F.; Huang, W.; Ginis, I. Hydrological modeling of storm runoff and snowmelt in Taunton River Basin by applications of HEC-HMS and PRMS models. *Nat. Hazards* **2018**, *91*, 179–199. [CrossRef]
4. Wang, N.; Lombardo, L.; Gariano, S.L.; Cheng, W.; Liu, C.; Xiong, J.; Wang, R. Using satellite rainfall products to assess the triggering conditions for hydro-morphological processes in different geomorphological settings in China. *Int. J. Appl. Earth Obs. Geoinf.* **2021**, *102*, 102350. [CrossRef]
5. Prakash, K.; Rawat, D.; Singh, S.; Chaubey, K.; Kanhaiya, S.; Mohanty, T. Morphometric analysis using SRTM and GIS in synergy with depiction: A case study of the Karmanasa River basin, North central India. *Appl. Water Sci.* **2019**, *9*, 13. [CrossRef]
6. Perucca, L.P.; Esper Angilieri, Y. Morphometric characterization of del Molle Basin applied to the evaluation of flash floods hazard, Iglesia Department, San Juan, Argentina. *Quat. Int.* **2011**, *233*, 81–86. [CrossRef]
7. Rai, P.K.; Singh, P.; Mishra, V.N.; Singh, A.; Sajan, V.; Shahi, A.P. Geospatial approach for quantitative drainage morphometric analysis of Varuna river basin, India. *J. Landsc. Ecol.* **2019**, *12*, 1–25. [CrossRef]
8. Rai, P.K.; Chandel, R.S.; Mishra, V.N.; Singh, P. Hydrological inferences through morphometric analysis of lower Kosi river basin of India for water resource management based on remote sensing data. *Appl. Water Sci.* **2018**, *8*, 15. [CrossRef]
9. Aher, P.; Adinarayana, J.; Gorantiwar, S. Quantification of morphometric characterization and prioritization for management planning in semi-arid tropics of India: A remote sensing and GIS approach. *J. Hydrol.* **2014**, *511*, 850–860. [CrossRef]
10. Shivhare, V.; Gupta, C.; Mallick, J.; Singh, C.K. Geospatial modelling for sub-watershed prioritization in Western Himalayan Basin using morphometric parameters. *Nat. Hazards* **2022**, *110*, 545–561. [CrossRef]
11. Abdeta, G.C.; Tesemma, A.B.; Tura, A.L.; Atlabachew, G.H. Morphometric analysis for prioritizing sub-watersheds and management planning and practices in Gidabo Basin, Southern Rift Valley of Ethiopia. *Appl. Water Sci.* **2020**, *10*, 158. [CrossRef]
12. Waiyasusri, K.; Chotpantarat, S. Watershed Prioritization of Kaeng Lawa Sub-Watershed, Khon Kaen Province Using the Morphometric and Land-Use Analysis: A Case Study of Heavy Flooding Caused by Tropical Storm Podul. *Water* **2020**, *12*, 1570. [CrossRef]
13. Ahirwar, R.; Malik, M.S.; Shukla, J.P. Prioritization of Sub-Watersheds for Soil and Water Conservation in Parts of Narmada River through Morphometric Analysis Using Remote Sensing and GIS. *J. Geol. Soc. India* **2019**, *94*, 515–524. [CrossRef]
14. Anees, M.T.; Abdullah, K.; Nawawi, M.; Rahman, N.N.N.A.; Ismail, A.Z.; Syakir, M.; Abdul Kadir, V. Prioritization of Flood Vulnerability Zones Using Remote Sensing and GIS for Hydrological Modelling. *Irrig. Drain.* **2019**, *68*, 176–190. [CrossRef]
15. Chauhan, P.; Chauniyal, D.D.; Singh, N.; Tiwari, R.K. Quantitative geo-morphometric and land cover-based micro-watershed prioritization in the Tons river basin of the lesser Himalaya. *Environ. Earth Sci.* **2016**, *75*, 498. [CrossRef]
16. Singh, G.; Pandey, A. Morphometric Characterization and Flash Flood Zonation of a Mountainous Catchment Using Weighted Sum Approach. In *Geospatial Technologies for Land and Water Resources Management*; Pandey, A., Chowdary, V.M., Behera, M.D., Singh, V.P., Eds.; Springer International Publishing: Berlin/Heidelberg, Germany, 2022; pp. 409–428. [CrossRef]
17. El-Fakharany, M.A.; Hegazy, M.N.; Mansour, N.M.; Abdo, A.M. Flash flood hazard assessment and prioritization of sub-watersheds in Heliopolis basin, East Cairo, Egypt. *Arab. J. Geosci.* **2021**, *14*, 1693. [CrossRef]
18. Jothimani, M.; Abebe, V.; Dawit, Z. Mapping of soil erosion-prone sub-watersheds through drainage morphometric analysis and weighted sum approach: A case study of the Kulfo River basin, Rift valley, Arba Minch, Southern Ethiopia. *Model. Earth Syst. Environ.* **2020**, *6*, 2377–2389. [CrossRef]
19. Mahmood, S.; Rahman, A. Flash flood susceptibility modeling using geo-morphometric and hydrological approaches in Panjkora Basin, Eastern Hindu Kush, Pakistan. *Environ. Earth Sci.* **2019**, *78*, 43. [CrossRef]
20. Mahmood, S.; Rahman, A. Flash flood susceptibility modelling using geomorphometric approach in the Ushairy Basin, eastern Hindu Kush. *J. Earth Syst. Sci.* **2019**, *128*, 97. [CrossRef]
21. Khan, I.; Bali, R.; Agarwal, K.K.; Kumar, D.; Singh, S.K. Morphometric Analysis of Parvati Basin, NW Himalaya: A Remote Sensing and GIS Based Approach. *J. Geol. Soc. India* **2021**, *97*, 165–172. [CrossRef]
22. Malik, A.; Kumar, A.; Kandpal, H. Morphometric analysis and prioritization of sub-watersheds in a hilly watershed using weighted sum approach. *Arab. J. Geosci.* **2019**, *12*, 118. [CrossRef]
23. Sakthivel, R.; Jawahar Raj, N.; Sivasankar, V.; Akhila, P.; Omine, K. Geo-spatial technique-based approach on drainage morphometric analysis at Kalrayan Hills, Tamil Nadu, India. *Appl. Water Sci.* **2019**, *9*, 24. [CrossRef]
24. Prasad, R.N.; Pani, P. Geo-hydrological analysis and sub watershed prioritization for flash flood risk using weighted sum model and snyder's synthetic unit hydrograph. *Model. Earth Syst. Environ.* **2017**, *3*, 1491–1502. [CrossRef]
25. Prakash, K.; Mohanty, T.; Singh, S.; Chaubey, K.; Prakash, P. Drainage morphometry of the Dhasan river basin, Bundelkhand craton, central India using remote sensing and GIS techniques. *J. Geomat.* **2016**, *10*, 122–132.
26. Kumar, A.; Singh, S.; Pramanik, M.; Chaudhary, S.; Maurya, A.K.; Kumar, M. Watershed prioritization for soil erosion mapping in the Lesser Himalayan Indian basin using PCA and WSA methods in conjunction with morphometric parameters and GIS-based approach. *Environ. Dev. Sustain.* **2022**, *24*, 3723–3761. [CrossRef]
27. Rahman, M.M.; Zaman, M.N.; Biswas, P.K. Optimization of significant morphometric parameters and sub-watershed prioritization using PCA and PCA-WSM for soil conservation: A case study in dharla River watershed, Bangladesh. *Model. Earth Syst. Environ.* **2022**, *8*, 2661–2674. [CrossRef]
28. Malik, A.; Kumar, A.; Kushwaha, D.P.; Kisi, O.; Salih, S.Q.; Al-Ansari, N.; Yaseen, Z.M. The Implementation of a Hybrid Model for Hilly Sub-Watershed Prioritization Using Morphometric Variables: Case Study in India. *Water* **2019**, *11*, 1505–1519. [CrossRef]

29. Meshram, S.G.; Sharma, S.K. Prioritization of watershed through morphometric parameters: A PCA-based approach. *Appl. Water Sci.* **2017**, *7*, 1505–1519. [CrossRef]
30. Meshram, S.G.; Alvandi, E.; Meshram, C.; Kahya, E.; Fadhil Al-Quraishi, A.M. Application of SAW and TOPSIS in Prioritizing Watersheds. *Water Resour. Manag.* **2020**, *34*, 715–732. [CrossRef]
31. CARE-Perú. *Modelización Hidrológica de la Cuenca Cañete y Evaluación del Impacto del Cambio Climático*; CARE-Perú: Lima, Peru, 2018.
32. Portuguez-Maurtua, M. Aplicación de la geoestadística a modelos hidrológicos en la cuenca del río Cañete. Master's Thesis, Universidad Nacional Agraria La Molina, Lima, Peru, 2017.
33. Arulbalaji, P.; Padmalal, D. Sub-watershed Prioritization Based on Drainage Morphometric Analysis: A Case Study of Cauvery River Basin in South India. *J. Geol. Soc. India* **2020**, *95*, 25–35. [CrossRef]
34. Meraj, G.; Romshoo, S.A.; Yousuf, A.R.; Altaf, S.; Altaf, F. Assessing the influence of watershed characteristics on the flood vulnerability of Jhelum basin in Kashmir Himalaya. *Nat. Hazards* **2015**, *77*, 153–175. [CrossRef]
35. Gajbhiye, S.; Mishra, S.K.; Pandey, A. Prioritizing erosion-prone area through morphometric analysis: An RS and GIS perspective. *Appl. Water Sci.* **2014**, *4*, 51–61. [CrossRef]
36. Odiji, C.A.; Aderoju, O.M.; Eta, J.B.; Shehu, I.; Mai-Bukar, A.; Onuoha, H. Morphometric analysis and prioritization of upper benue river watershed. *Appl. Water Sci.* **2021**, *11*, 41. [CrossRef]
37. Strahler, A. Quantitative Geomorphology of Drainage Basin and Channel Networks. In *Handbook of Applied Hydrology*; McGraw-Hill: New York, NY, USA, 1964.
38. Horton, R.E. Erosional development of streams and their drainage basins; hydrophysical approach to quantitative morphology. *Geol. Soc. Am. Bull.* **1945**, *56*, 275–370. [CrossRef]
39. Nooka Ratnam, K.; Srivastava, Y.; Venkateswara Rao, V.; Amminedu, E.; Murthy, K. Check dam positioning by prioritization of micro-watersheds using SYI model and morphometric analysis remote sensing and GIS perspective. *J. Indian Soc. Remote Sens.* **2005**, *33*, 25–38. [CrossRef]
40. Sreedevi, P.D.; Sreekanth, P.D.; Khan, H.H.; Ahmed, S. Drainage morphometry and its influence on hydrology in an semi arid region: Using SRTM data and GIS. *Environ. Earth Sci.* **2013**, *70*, 839–848. [CrossRef]
41. Schumm, S.A. Evolution of drainage systems and slopes in badlands at Perth Amboy, New Jersey. *Geol. Soc. Am. Bull.* **1956**, *67*, 597–646. [CrossRef]
42. Horton, R.E. Drainage-basin characteristics. *Trans. Am. Geophys. Union* **1932**, *13*, 350–361. [CrossRef]
43. Miller, V. A Quantitative Geomorphic Study of Drainage Basin Characteristics in the Clinch Mountain Area Virginia and Tennessee. *J. Geol.* **1953**, *65*, 112–113. [CrossRef]
44. Farr, T.G.; Rosen, P.A.; Caro, E.; Crippen, R.; Duren, R.; Hensley, S.; Kobrick, M.; Paller, M.; Rodriguez, E.; Roth, L.; et al. The Shuttle Radar Topography Mission. *Rev. Geophys.* **2007**, *45*, 5326–5350. [CrossRef]
45. Amani, M.; Ghorbanian, A.; Ahmadi, S.A.; Kakooei, M.; Moghimi, A.; Mirmazloumi, S.M.; Moghaddam, S.H.A.; Mahdavi, S.; Ghahremanloo, M.; Parsian, S.; et al. Google Earth Engine Cloud Computing Platform for Remote Sensing Big Data Applications: A Comprehensive Review. *IEEE J. Sel. Top. Appl. Earth Obs. Remote Sens.* **2020**, *13*, 5326–5350. [CrossRef]
46. Mutanga, O.; Kumar, L. Google Earth Engine Applications. *Remote Sens.* **2019**, *11*, 18–27. [CrossRef]
47. Gorelick, N.; Hancher, M.; Dixon, M.; Ilyushchenko, S.; Thau, D.; Moore, R. Google Earth Engine: Planetary-scale geospatial analysis for everyone. *Remote Sens. Environ.* **2017**, *202*, 18–27. [CrossRef]
48. Zhao, Q.; Yu, L.; Li, X.; Peng, D.; Zhang, Y.; Gong, P. Progress and Trends in the Application of Google Earth and Google Earth Engine. *Remote Sens.* **2021**, *13*, 3778. [CrossRef]
49. Tamiminia, H.; Salehi, B.; Mahdianpari, M.; Quackenbush, L.; Adeli, S.; Brisco, B. Google Earth Engine for geo-big data applications: A meta-analysis and systematic review. *ISPRS J. Photogramm. Remote Sens.* **2020**, *164*, 152–170. [CrossRef]
50. Konrad Banachewicz, L.M. *The Kaggle Book*; Packt: Birmingham, UK, 2022; ISBN 9781801817479.
51. Ismail, M.; Singh, H.; Farooq, I.; Yousuf, N. Quantitative morphometric analysis of Veshav and Rembi Ara watersheds, India, using quantum GIS. *Appl. Geomat.* **2022**, *14*, 119–134. [CrossRef]
52. Basnet, K.; Paudel, R.C.; Sherchan, B. Analysis of watersheds in Gandaki province, Nepal using QGIS. *Tech. J.* **2019**, *1*, 16–28. [CrossRef]
53. Alencar da Silva Alves, K.M.; Parodi Dávila, M.C.; Zimmermann García, E.D.; Rodrigues de Lira, D.; De Araujo Monteiro, K. Caracterización morfométrica de la cuenca del Salado Bajo, Región de Atacama, Chile. *Investig. Geográficas* **2021**, *62*, 90–105. [CrossRef]
54. Gayen, S.; Bhunia, G.S.; Shit, P.K. Morphometric Analysis of Kangshabati-Darkeswar Interfluves Area in West Bengal, India using ASTER DEM and GIS Techniques. 2013. Available online: http://111.93.204.14:8080/xmlui/handle/123456789/582 (accessed on 30 November 2022).